# nature climate change

**Article** 

https://doi.org/10.1038/s41558-023-01600-z

# Net loss of biomass predicted for tropical biomes in a changing climate

Received: 18 January 2022

Accepted: 6 January 2023

Published online: 06 February 2023



Check for updates

Maria del Rosario Uribe <sup>1,2</sup> ✓, Michael T. Coe <sup>3</sup>, Andrea D. A. Castanho <sup>3</sup>, Marcia N. Macedo 1, Denis Valle 4 & Paulo M. Brando 1,2,5

Tropical ecosystems store over half of the world's aboveground live carbon as biomass, and water availability plays a key role in its distribution. Although precipitation and temperature are shifting across the tropics, their effect on biomass and carbon storage remains uncertain. Here we use empirical relationships between climate and aboveground biomass content to show that the contraction of humid regions, and expansion of those with intense dry periods, results in substantial carbon loss from the neotropics. Under a low emission scenario (Representative Concentration Pathway 4.5) this could cause a net reduction of above ground live carbon of ~14.4–23.9 PgC (6.8–12%) from 1950–2100. Under a high emissions scenario (Representative Concentration Pathway 8.5) net carbon losses could double across the tropics, to ~28.2-39.7 PgC (13.3-20.1%). The contraction of humid regions in South America accounts for ~40% of this change. Climate mitigation strategies could prevent half of the carbon losses and help maintain the natural tropical net carbon sink.

Tropical ecosystems span 54 million km<sup>2</sup>, storing over 50% of the world's aboveground live carbon as biomass<sup>1-3</sup>. Precipitation and temperature are the underlying variables driving processes that directly and indirectly influence the amount of carbon assimilation and storage in tropical ecosystems. Under a stable climate, warm and wet climate zones house carbon-rich tropical forests, while more arid climate zones store lower amounts of carbon as biomass. Climate changes may disrupt these steady-state patterns, shifting the capacity of these ecosystems to assimilate and store carbon—and potentially releasing some of the ~193–229 Pg of aboveground carbon stored in the tropics to the atmosphere 1,2. Even a partial release of this carbon would accelerate global warming.

How much carbon tropical biomes will store in the future remains an open question. With climate change, tropical biomes could either gain or lose carbon throughout this century<sup>4-11</sup>. Major uncertainties in current projections relate to how Earth System Models (ESMs) represent interactions among droughts, heat stress and CO<sub>2</sub> fertilization in carbon-rich forested ecosystems<sup>5,6,8-10</sup>. For example, some ESMs lack the ability to mimic natural disturbances related to drought-, wind- and heat-related tree mortality<sup>12,13</sup>. Most ESMs are also overly sensitive to CO<sub>2</sub> fertilization<sup>14,15</sup>, which minimizes modelled climate change effects on forest carbon dynamics. Empirical relationships between vegetation structure and climate can thus provide valuable insights into the potential effects of climate change on the distribution of tropical biomes and their future carbon storage capacity.

Empirical models capture the equilibrium outcome of complex interactions and processes lacking in most ESMs. Recent studies have applied the empirical relationships between precipitation and current biome distributions to model climate-induced shifts in humid tropical forests during the coming century both in the Amazon<sup>16</sup> and globally<sup>17</sup>. Other studies have used the relationship between precipitation, potential evapotranspiration and biome distribution to predict a substantial expansion of drylands this century<sup>18</sup>, as well as decreases in aboveground biomass (AGB) in seasonally dry tropical forests<sup>19</sup>.

In this study, we use empirical climate relationships and AGB data  $(Baccini\,et\,al.^2, Xu\,et\,al.^3\,and\,Santoro\,and\,Cartus^{20})\,to\,quantify\,the\,scale$ of potential changes in tropical AGB and carbon that can be expected under climate change, following the 4.5 and 8.5 Representative

Department of Earth System Science, University of California Irvine, Irvine, CA, USA. 2Yale School of the Environment, Yale University, Yale, CT, USA. <sup>3</sup>Woodwell Climate Research Center, Falmouth, MA, USA. <sup>4</sup>School of Forest, Fisheries, and Geomatics Sciences, University of Florida, Gainesville, FL, USA. ⁵Instituto de Pesquisa Ambiental da Amazônia (IPAM), Brasília-DF, Brazil. ⊠e-mail: rosariouribed@gmail.com; paulo.brando@yale.edu

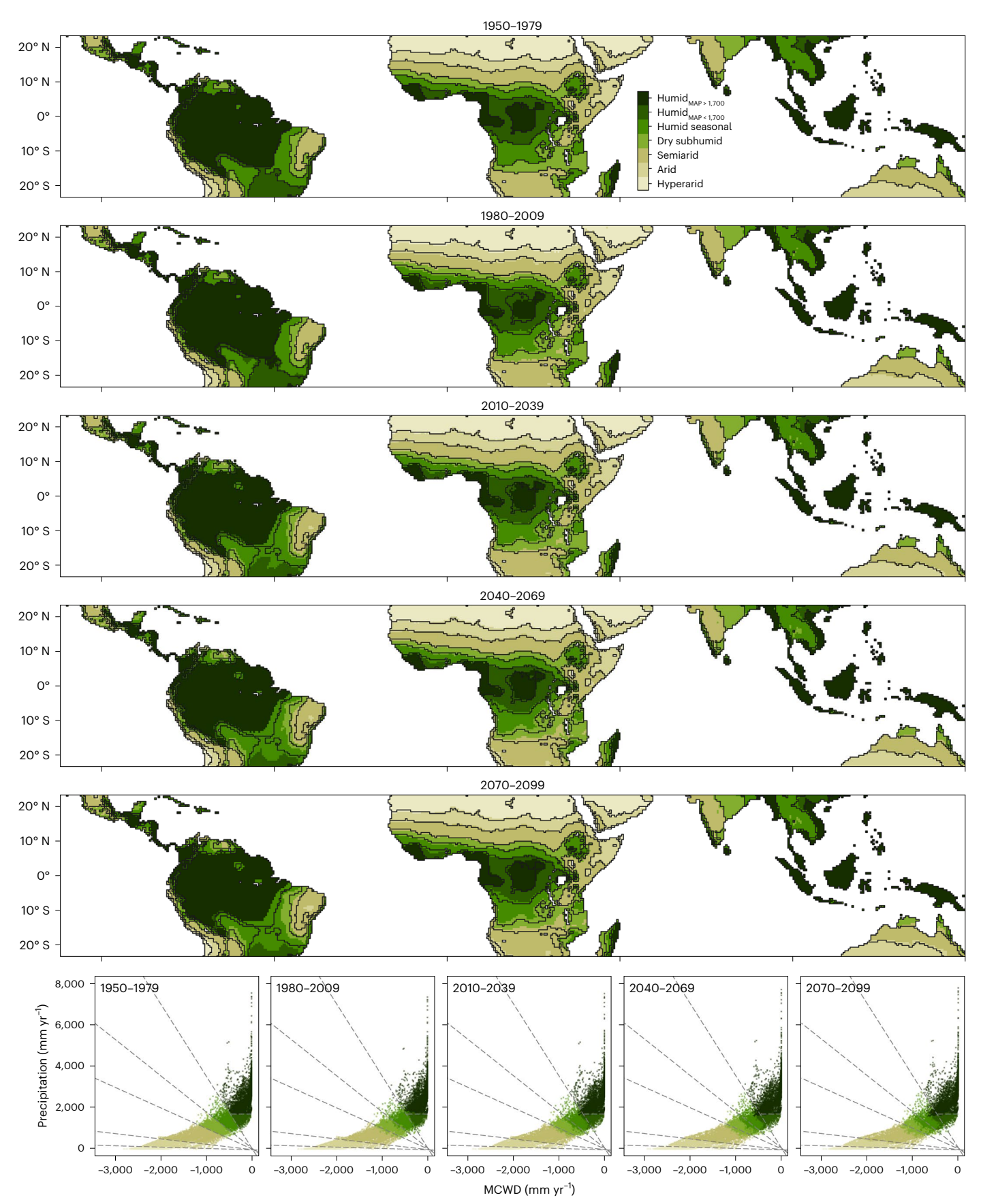
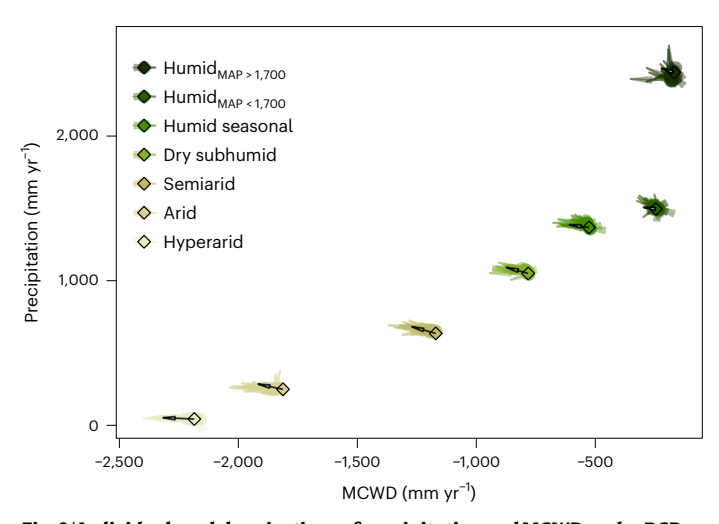


Fig. 1 | Distribution of climatic zones in the tropics for historic and future 30-year time periods (1950–1979, 1980–2009, 2010–2039, 2040–2069 and 2070–2099) under RCP 4.5. Colours represent the climatic zones. Contour lines in the maps and grey dashed lines in the scatterplots are plotted for reference to show

the distribution and limits of the climatic zones in the period 1950–1979. Climate data from CRU v.4.04 (ref.  $^{45}$ ) for 1950–2009 and from CMIP5 projections  $^{46,47}$  for 2010–2099 under RCP 4.5.



**Fig. 2**| **Individual model projections of precipitation and MCWD under RCP 4.5.** Dots represent each model's mean historic (1950–1979) climate for each climatic zone. Connected arrowheads represent average climate at the end of the century (2070–2099). The black shapes correspond to the average climate from all models. Models used are listed in Supplementary Table 1. Climate data for 1950–2009 are from CRU v.4.04 (ref. <sup>45</sup>). Data for 2010–2099 are from CMIP5 projections <sup>46,47</sup> under RCP 4.5.

Concentration Pathways (RCPs). We address the following questions: (1) What are the relationships between current climatic zones (from hyperarid to humid) and biomass across the entire tropics? (2) What are the predicted changes in distribution of these climatic zones during the twenty-first century? (3) What are the expected changes in biomass and carbon stocks associated with those projected changes? Our assumption is that AGB is currently at equilibrium with climate 16,17 and that vegetation will equilibrate to match projected climate changes at some time in the future. Based on this approach, we can estimate how much carbon may be gained or lost by the end of this century throughout the tropics. We used two different methods to estimate AGB changes: the first is a discrete model based on average biomass in each climate zone and the second is a continuous model based on quantile regression forests (Methods). For simplicity, our results focus on the discrete model, using RCP 4.5 as our current pathway, while commenting briefly on the quantile regression forests and RCP 8.5 predictions. For complete results, refer to Extended Data Figs. 1-4.

#### Climate change and climatic zones in the tropics

We categorized climatic zones based on their location in the climate space, defined by average annual precipitation and the maximum climatological water deficit (MCWD)—a measure of how temperature and precipitation influence the intensity of the dry season or dry periods (Methods) (Fig. 1 (lower panel) and Supplementary Table 2). From 1980–2009, about one third (-34.1%) of the tropics was characterized by a humid climate, where tropical forests are common (Supplementary Table 3). Almost half (-45.3%) of the tropics was in the humid seasonal, dry subhumid and semiarid climate zones, where seasonally dry tropical forests, savannas and grasslands dominate. Arid and hyperarid zones covered the remaining -20.5%, occupied mostly by deserts and seasonal grasslands.

Climate model results point to an ongoing shift in the climate space of the tropics, primarily driven by increased MCWD (Figs. 1 and 2 and Extended Data Figs. 1 and 2), with all climate models projecting more intense dry periods in both scenarios RCP 4.5 (Fig. 2) and RCP 8.5 (Extended Data Fig. 2 and Supplementary Fig. 1). The increase in MCWD is more severe in arid lands compared with wetter climatic zones. In contrast, projected changes in precipitation are more variable across

models and climatic zones. For instance, more than one-third of the Coupled Model Intercomparison Project Phase 5 (CMIP5) climate models predict less precipitation in the wettest tropical regions (that is, humid zone with mean annual precipitation (MAP) above 1,700 mm, or humid  $_{\text{MAP} > 1700}$ ), but most predict increased precipitation for all other climatic zones. Regionally, decreases in precipitation are concentrated in the Americas, while increases are more widespread in Africa, Asia and Oceania (Supplementary Fig. 2). Overall, the magnitude of changes in precipitation (that is, the length of the arrows in Fig. 2) is lower compared to MCWD, regardless of the direction of change.

The drier and hotter climate in the tropics results in an overall loss of humid climate zones and associated gains in arid zones (Fig. 3). Our results suggest that historical climatic changes (1950–2009) have already favoured a slight expansion of hyperarid, arid and semiarid areas (1.5%) over the dry subhumid and three humid climate zones (Fig. 3 and Supplementary Table 4).

As climate changes further, humid climate zones (humid  $_{MAP>1,700}$ , humid  $_{MAP>1,700}$  and humid seasonal) are projected to shrink from 48.9% (1950–1979) to 46.1% (2040–2069) and 45.7% (2070–2099) of the tropics. From 1950–2099, the humid  $_{MAP>1,700}$  and humid  $_{MAP<1,700}$  zones could decline by 1.1 and 2.8% respectively, while humid seasonal areas could expand by 0.6%. A 4.2% reduction in the Americas accounts for most of the projected decline in the humid  $_{MAP>1,700}$  (typically occupied by rainforests), in contrast to a projected 0.6% expansion in tropical Africa.

The net changes in area of each climate zone are relatively small compared with the many shifts in their distribution during the study period. On average, 19.6% of the tropics shifted its climate zone at some point between 1950-1979 and 2070-2099 (Fig. 3 and Table 1). For instance, the  $humid_{MAP<1,700}$  has a predicted net change in area of 2.8% from 1950-2100, but about 42.4% of its historic (1950-1979) area will change climate zones at least once by 2100. For the humid seasonal and dry subhumid zones, ~34% of the area will change. Even in climatic zones with fewer shifts, we find that ~10% of the region will change to a different climatic zone by the end of the century. Moreover, about 6.9% of the tropics will experience more than one shift in equilibrium climate from 1950-2100, mostly in the humid seasonal and humid<sub>MAP>1.700</sub> climate zones. Thus, relatively small net changes in area (1950-2100) may mask complex dynamics, including where large swaths of a given climatic zone are projected to transition to or from other climatic zones by 2100. Most of these transitions are likely to favour drier climatic zones (Table 1).

#### Changes in above ground biomass and carbon

Given that the climate space determines much of the AGB distribution (that is, higher rainfall and MCWD are associated with higher biomass) (Fig. 4a), changes in the climate space may lead to changes in the equilibrium biomass (Fig. 4b). Climatic conditions over the past 50 years point to a total decrease in equilibrium biomass of  $-3.09 \pm 2.62$  PgC, representing -1.5% of total carbon in 1950 (Fig. 4b and Supplementary Table 5). These small changes in biomass and carbon are due mainly to losses in arid and semiarid zones that shifted to drier climates. Most potential carbon losses from 1950–2009 were concentrated in Africa (Fig. 5).

According to our discrete model, future changes in climate under RCP 4.5 will probably force additional transitions from higher to lower biomass climate zones. We find an expected net reduction in equilibrium AGB carbon of about  $-14.38\pm2.38$  PgC, representing a  $-6.8\pm1.1\%$  loss compared to 1950 (-0.1 PgC yr $^{-1}$ ). Using a quantile regression forest (QRF) modelling approach, we found similar spatial and temporal patterns but higher absolute losses (Supplementary Tables 7 and 8). For instance, from 1950-2100 the QRF approach projected C losses of  $-23.88\pm2.35$  PgC (Extended Data Fig. 3b). These higher projected losses were mainly attributed to regions (pixels) that moved to a lower equilibrium biomass but stayed within the same climatic zone. In our discrete approach, these regions were projected to maintain the same

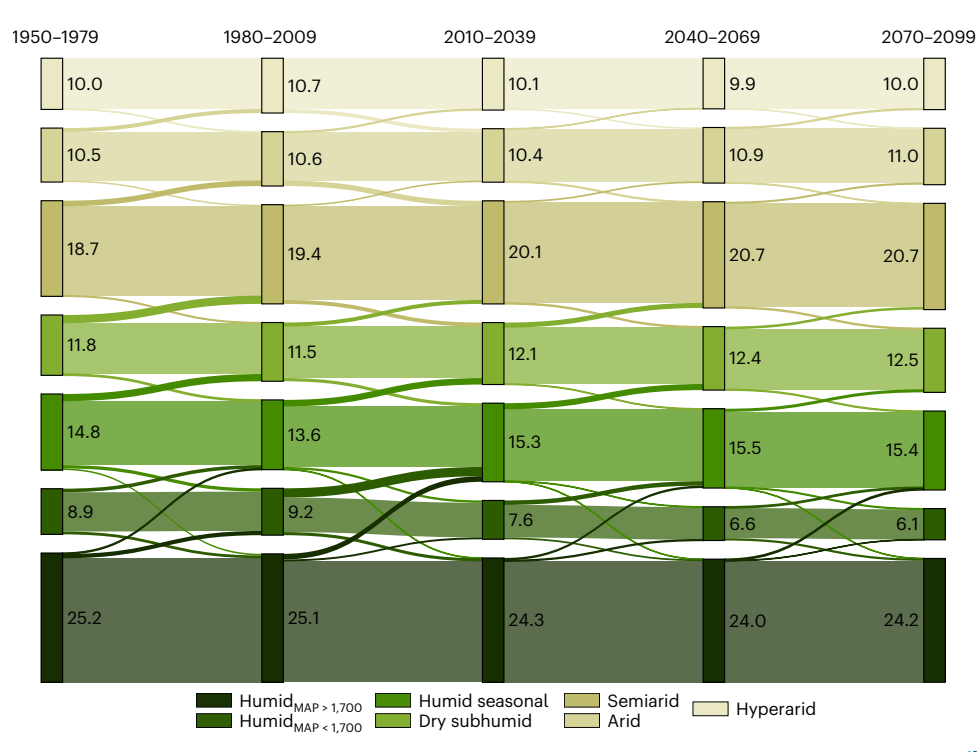


Fig. 3 | Percentage changes in area covered by each climatic zone from 1950–2099. Climate data for 1950–2009 are from CRU v.4.04 (ref. <sup>45</sup>). Data for 2010–2099 are from CMIP5 projections <sup>46,47</sup> under RCP 4.5.

equilibrium biomass. The expected changes (losses and gains) in area for the different climatic zones are fairly constant between 1950 and 2100, with no abrupt changes in the rate of net carbon losses.

By 2100, the largest potential AGB and carbon losses are likely to occur with the contraction of humid climates, where carbon-dense evergreen and drought deciduous forests store ~157.02 PgC (155.55–158.39 PgC)—the largest fraction (74%) of the carbon pool in the tropics. These humid climatic zones would lose more carbon than any other zone (~8.44 and ~10.58 PgC in humid\_MAP>1,700 and humid\_MAP<1,700, respectively). The largest carbon increases are in semiarid and humid seasonal regions (+1.03 and +2.53 PgC, respectively). However, these increases are too small to offset the much larger expected losses of equilibrium AGB and carbon from more humid climatic zones. With the QRF model, losses from the humid\_MAP>1,700 and humid\_MAP<1,700 climatic zones are around ~15.15 and ~9.1 PgC, respectively.

Shifts in the tropical average distribution of climatic zones mask important changes in biomass within specific tropical regions. For instance, projected net biomass changes in the humid  $_{\rm MAP}>1,700$  reflect losses in the Americas and Asia (–8.36 and –1.04 PgC, respectively) being compensated by gains in Africa (+1 PgC). In fact, total equilibrium carbon losses for the Americas could be as high as –10.5 PgC by the end of the century, while losses in Africa and Asia are smaller (–2.07 and –1.74 PgC, respectively). Potential carbon gains are concentrated in the humid seasonal zone in Asia and the Americas, and in the humid  $_{\rm MAP}>1,700$  in Africa. Regional patterns of C changes were similar between our two methods (that is, the discrete method and the QRF), but our QRF approach shows higher C losses in all regions.

The variation in climate predictions in the models drives some uncertainty in changes in equilibrium biomass. Under the RCP 8.5 scenario, the equilibrium carbon losses nearly double compared to those of RCP 4.5, corresponding to losses of about  $-28.24 \pm 2.24$  PgC, or  $-13.3 \pm 1.1\%$  of pantropical C in 1950 (-0.19 PgC yr<sup>-1</sup>) (Supplementary Table 6 and Extended Data Figs. 3c and 4). In the QRF model, carbon losses under RCP 8.5 reach  $-39.71 \pm 2.23$  PgC, or  $-20.1 \pm 1.3\%$  of pantropical C in 1950 (-0.26 PgC yr<sup>-1</sup>) (Extended Data Fig. 4d). Changes

Table 1 | Changes in climatic zones over the study period (baseline 1950–1979)

| Climatic zone                     | Changed area (%) | Unchanged<br>area (%) | Change to<br>a more arid<br>zone (%) | Change to a<br>more humid<br>zone (%) |
|-----------------------------------|------------------|-----------------------|--------------------------------------|---------------------------------------|
| (1) Hyperarid                     | 4.9              | 95.1                  | -                                    | 3.4                                   |
| (2) Arid                          | 15.1             | 84.9                  | 3.7                                  | 3.0                                   |
| (3) Semiarid                      | 11.2             | 88.8                  | 4.6                                  | 1.7                                   |
| (4) Dry subhumid                  | 34.0             | 66.0                  | 24.7                                 | 1.7                                   |
| (5) Humid<br>seasonal             | 34.3             | 65.7                  | 23.8                                 | 1.5                                   |
| (6) Humid <sub>MAP&lt;1,700</sub> | 42.4             | 57.6                  | 30.7                                 | 7.1                                   |
| (7) Humid <sub>MAP&gt;1,700</sub> | 10.3             | 89.7                  | 6.9                                  | -                                     |
| All climatic zones                | 19.6             | 80.4                  | -                                    | -                                     |

Columns 2 and 3: area (%) of each climatic zone that changed, or is projected to change (or not), at some point between 1950 and 2100. Columns 4 and 5: area (%) of each climatic zone that changed, or is projected to change, to a more arid or more humid zone by 2100. Climate data from CRU v.4.04 (ref.  $^{45}$ ) for 1950–2009 and from CMIP5 projections  $^{46,47}$  for 2010–2099 under RCP 4.5

in carbon (by region and climate zone) are similar to those observed in the RCP 4.5 scenario, but of greater magnitude. The largest carbon losses are in the humid  $_{\rm MAP>1,700}$  and humid  $_{\rm MAP<1,700}$  climate zones in the Americas, which together lose  $-20.81\pm1.4$  PgC or  $-25.9\pm1.5$  PgC (based on the QRF results).

#### **Discussion**

Our results show that climate change is driving a large part of the tropics out of its historical biomass equilibrium, primarily by increasing dry-season severity. Regions with a humid climate and high AGB concentrations today will likely experience more severe dry seasons by

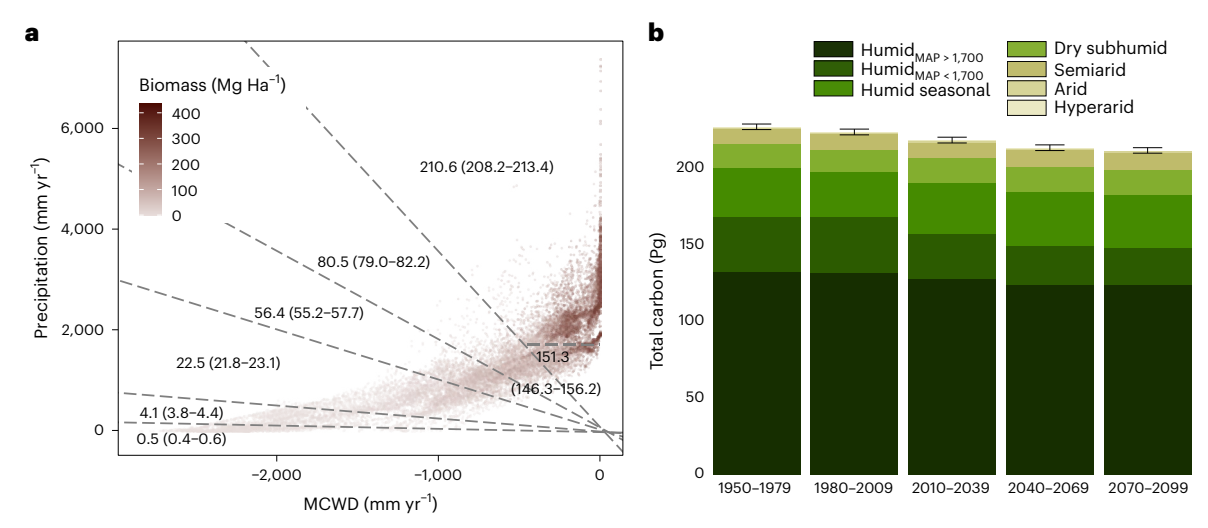


**Fig. 4** | **Biomass and biomass changes across the tropics under RCP 4.5. a**, Average AGB density (from the three AGB datasets) $^{2,3,20}$  of each pixel (colour scale) across the tropics in Mg ha $^{-1}$  plotted in climate space (P versus MCWD). Numbers indicate the average AGB density and numbers in parentheses indicate the confidence limits (from non-parametric bootstrapping) for the AGB density in each climatic zone. The number in the right bottom corner corresponds to the

humid $_{MAP<1,700}$  (151.3 (145.3–156.2) Mg Ha $^{-1}$ ). **b**, Changes in carbon (Pg) by climatic zone from 1950–2099. Bar height is the average total C in each timeframe  $\pm$  the bootstrapped confidence limits (that is, average of 1,000 samples of predicted C for each timestep). Climate data come from CRU v.4.04 (ref.  $^{45}$ ) for 1950–2009 and from CMIP5 projections  $^{46,47}$  for 2010–2099 under RCP 4.5.

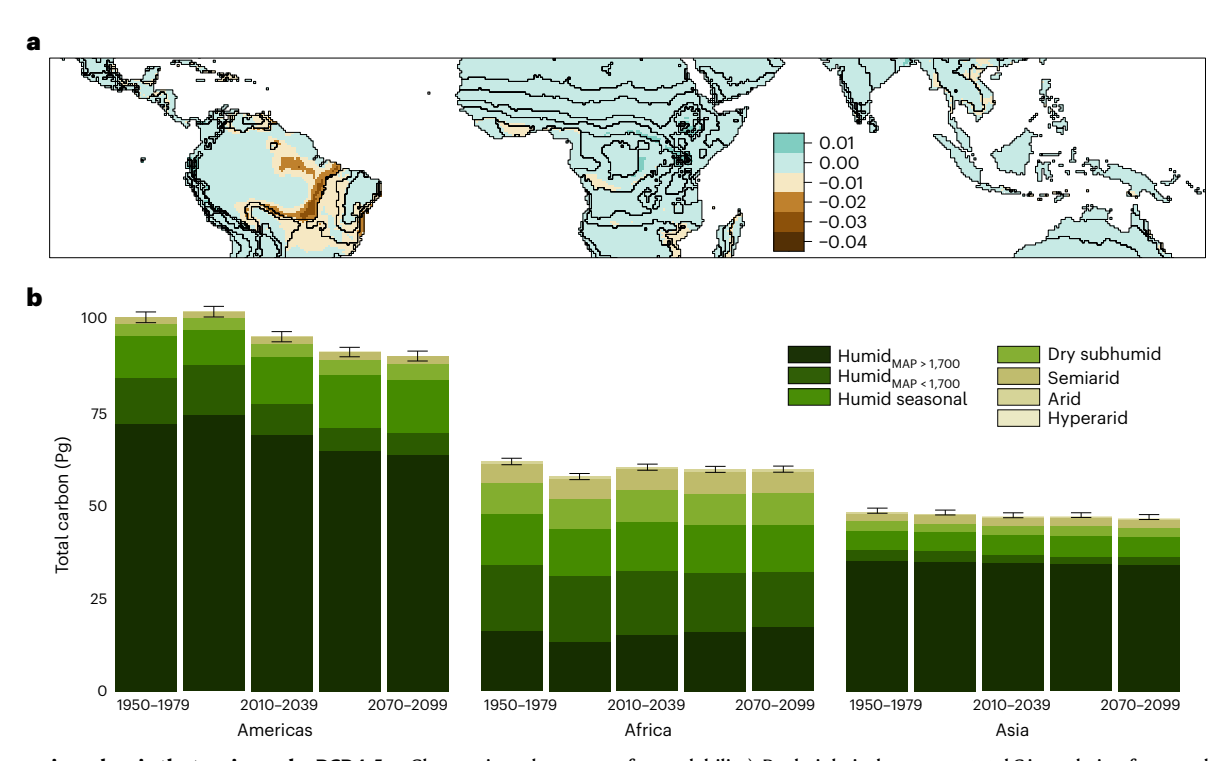


**Fig. 5** | **Changes in carbon in the tropics under RCP 4.5. a**, Changes in carbon levels (in Pg) by pixel. The contour lines in **a** correspond to the distribution of the climatic zones in 1950 as shown in Fig. 1. **b**, Changes in carbon levels (in Pg) by climatic zone and by region from 1950–2099 (only three timesteps labelled

for readability). Bar height is the average total C in each timeframe  $\pm$  the bootstrapped confidence limits (that is, average of 1,000 samples of predicted C for each timestep). Climate data from CRU v.4.04 (ref.  $^{45}$ ) for 1950–2009 and from CMIP5 projections  $^{46,47}$  for 2010–2099 under RCP 4.5.

2100. These climatic changes could eventually lead to losses between 14.4 and 23.9 PgC (0.1–0.16 PgC yr $^{\!-1}$ ) across the tropics under RCP 4.5. The lower estimate is from a discrete empirical model, while the higher estimate is from a QRF that captures changes in equilibrium biomass driven by smaller changes in climate. Predicted carbon losses

are even higher if  $CO_2$  emissions follow the worst-case scenario (RCP 8.5). According to predictions for RCP 8.5 using the QRF approach, carbon losses could be as high as 39.7 PgC (0.26 PgC yr<sup>-1</sup>). For comparison, the net tropical carbon sink of intact tropical forests averaged 0.08–0.78 PgC yr<sup>-1</sup> from 2000–2014<sup>21</sup>. Gross carbon losses (including

all types of disturbances) from tropical forests over the same period were estimated at 0.81–0.88 PgC yr<sup>-1</sup> (ref. <sup>21</sup>).

Estimates from our discrete model indicate that carbon losses are concentrated in the Americas (10.5 PgC), where the humid regions shrink by 4.2%. Changes in Africa and Asia are much smaller because they contain less carbon and the projected regional drying is less severe. This divergent redistribution of climatic zones results in a relatively small decrease in total carbon throughout the African continent. In Asia, the projected redistribution of climatic zones and changes in biomass are even smaller.

Our predicted declines in equilibrium AGB and tropical carbon stocks generally agree with observed trends in carbon losses attributed to climate change, particularly droughts<sup>22-24</sup>. In intact forests, for instance, field-based observations and predictions indicate recent or near-term declines in biomass accumulation during episodic droughts<sup>25-27</sup>. The reduction in carbon sequestration in these intact forests was associated with extreme droughts<sup>23,26</sup>, when air temperature was often substantially higher than historical values. Several studies also predict that forest degradation and fires will increase carbon losses in humid tropical regions, which can accelerate during unusually dry and warm years<sup>3,23,28</sup>.

Because our empirical approach does not capture other potential effects of future climate changes (for example, direct temperature effects, lightning or wind throw)  $^{8,29-33}$  or anthropogenic factors (for example, changes in fire, deforestation and forest degradation patterns)  $^{24,34,35}$ , it likely underestimates changes in tropical carbon stocks. Conversely, natural and anthropogenic biomass recovery (forest thickening,  $\rm CO_2$  fertilization, reforestation and afforestation initiatives)  $^{10,36,37}$  processes, which are not captured here, could partially mitigate our predicted carbon losses.

Although we found that dry-warm future conditions would likely reduce carbon storage, many ESMs predict long-term increases in AGB in tropical forests  $^{10}$ . CO $_2$  fertilization is the main process accounting for these differences between our empirical approach and ESMs. The debate about CO $_2$  fertilization is still ongoing, with some observational evidence of CO $_2$  fertilization increasing tropical forest carbon stocks  $^{25,26}$  while recent field-based studies suggest that the rate of carbon gain is slowing  $^{12,25,26}$ . Moreover, other processes that reduce the vegetation carbon sink are frequently misrepresented in ESMs, including nutrient limitation, drought vulnerability, plant mortality, biomass turnover and fire disturbance  $^{11,14,15,37,38,39,40}$ . Here, we estimate important carbon losses based on the historic association between climate and biotic factors, but we do not account for potential novel effects of CO $_2$  fertilization on the relationship between climate, AGB and carbon stocks.

In regions dominated by tropical savannas, some studies predict increased carbon stocks due to ( $\mathrm{CO}_2$  fertilization-driven) woody encroachment<sup>3,9,41</sup>. We also predict slight carbon increases in the climate zone associated with savannas, but primarily due to the expansion of savanna climate zones into historically forested regions. Even if woody encroachment became more common in this expanded savanna climate zone, the increase in biomass would be much less than that of the forests they replaced. Changes in fire frequency and intensity will also play a key role in carbon dynamics and the potential for woody encroachment in savannas<sup>28,38</sup>. More frequent and more intense fires are predicted under climate change—a direct threat to tree saplings and woody plant growth that could trigger major carbon losses.

According to our estimates, 5.9-9.8 PgC would be lost from tropical vegetation for each  $1\,^{\circ}$ C increase in global temperature (under the RCP 4.5 scenario). Temperature directly affects carbon storage and it is likely that tropical forests are already nearing a temperature threshold  $^{26,39,42}$ . Photosynthesis (and hence carbon uptake) saturates with small increases in temperature  $^{43}$  in tropical forest ecosystems—a process that could accelerate if higher temperatures are accompanied by more intense droughts that reduce soil moisture and allow more frequent and intense fires.

Although we predicted small net changes in climate zone extents under future climate, this result masks complex shifts in their spatial distribution over time. Despite only modest (<10%) changes in the total area of each zone, we find that 19.6% of the entire tropics will move into another climate space and almost 42.4% of the humid zone (MAP < 1,700) typically occupied by seasonal or transitional forests will change its equilibrium climate at least once before 2100. During these transitions, gross carbon emissions from vegetation diebacks could be much larger than the net equilibrium loss of ~14.4–23.9 PgC presented here. Plant adaptations to future climatic conditions could also modify the empirical relationship between biomass and climate, thus reducing carbon losses. Improving estimates of how rapidly plants could adapt to new climatic conditions represents a key area for future research

The changes in tropical biomass predicted here could further increase atmospheric  $\mathrm{CO}_2$  concentrations, prompting positive vegetation–atmosphere feedbacks. The humid climate zones predicted to experience the greatest losses are also home to dense tropical forests responsible for about 22% of net terrestrial carbon sequestration<sup>22</sup>. As these zones shrink, we will not only lose their standing stock but also an important part of the terrestrial carbon sink. Tropical biomass dynamics may also be influenced by climate changes due to the biophysical effects of  $\mathrm{CO}_2$  fertilization and deforestation<sup>44</sup>. For instance, forests in the eastern Amazon, where large biomass losses are expected, exert a strong positive feedback on precipitation through  $\mathrm{CO}_2$ -induced changes in stomatal conductance. Decreased biomass could therefore reduce precipitation in the same region and further accelerate carbon losses<sup>44</sup>.

Ongoing (and often irreversible) human-induced changes in biomass, including land-cover change, forest degradation and ecosystem fragmentation, are causing large and rapid losses of carbon throughout the tropics  $^{23,24,34}$ . For instance, carbon losses from deforestation and forest degradation were about  $-0.07\ PgC\ yr^{-1}$  in the Brazilian Amazon alone from  $2010-2019^{24}$ , compared with  $-0.17\ PgC\ yr^{-1}$  in the entire Amazon basin from  $2001-2015^{34}$ . The interactions between anthropogenic disturbances and climate change could result in additional important losses of carbon stocks and a reduction (or reversal) of the natural tropical carbon sink  $^{8,12,24}$ . Protecting key biomes and their associated carbon stocks will therefore require reducing the rate of such anthropogenic disturbances in addition to lowering global GHG emissions. Moreover, our analyses demonstrate that reducing GHG emissions from RCP 8.5 to 4.5 would mitigate climate-driven carbon losses by about a half.

#### **Online content**

Any methods, additional references, Nature Portfolio reporting summaries, source data, extended data, supplementary information, acknowledgements, peer review information; details of author contributions and competing interests; and statements of data and code availability are available at https://doi.org/10.1038/s41558-023-01600-z.

#### References

- Saatchi, S. S. et al. Benchmark map of forest carbon stocks in tropical regions across three continents. Proc. Natl Acad. Sci. 108, 9899–9904 (2011).
- Baccini, A. et al. Estimated carbon dioxide emissions from tropical deforestation improved by carbon-density maps. *Nat. Clim.* Change 2, 182–185 (2012).
- 3. Xu, L. et al. Changes in global terrestrial live biomass over the 21st century. Sci. Adv. 7, eabe9829 (2021).
- Betts, R. A. et al. The role of ecosystem-atmosphere interactions in simulated Amazonian precipitation decrease and forest dieback under global climate warming. *Theor. Appl. Climatol.* 78, 157–175 (2004).

- Cox, P. M. et al. Sensitivity of tropical carbon to climate change constrained by carbon dioxide variability. *Nature* 494, 341–344 (2013).
- Rammig, A. et al. Estimating the risk of Amazonian forest dieback. N. Phytol. 187, 694–706 (2010).
- 7. Huntingford, C. et al. Towards quantifying uncertainty in predictions of Amazon 'dieback'. *Philos. Trans. R. Soc. B Biol. Sci.* **363**, 1857–1864 (2008).
- Galbraith, D. et al. Multiple mechanisms of Amazonian forest biomass losses in three dynamic global vegetation models under climate change. N. Phytol. 187, 647–665 (2010).
- Kumar, D., Pfeiffer, M., Gaillard, C., Langan, L. & Scheiter, S. Climate change and elevated CO2 favor forest over savanna under different future scenarios in South Asia. *Biogeosciences* 18, 2957–2979 (2021).
- Huntingford, C. et al. Simulated resilience of tropical rainforests to CO2-induced climate change. *Nat. Geosci.* 6, 268–273 (2013).
- Brienen, R. J. W. et al. Forest carbon sink neutralized by pervasive growth-lifespan trade-offs. Nat. Commun. 11, 4241 (2020).
- Koch, A., Hubau, W. & Lewis, S. L. Earth system models are not capturing present-day tropical forest carbon dynamics. *Earths Future* 9, e2020EF001874 (2021).
- Negrón-Juárez, R. I., Koven, C. D., Riley, W. J., Knox, R. G. & Chambers, J. Q. Observed allocations of productivity and biomass, and turnover times in tropical forests are not accurately represented in CMIP5 Earth system models. *Environ. Res. Lett.* 10, 064017 (2015).
- Fleischer, K. et al. Amazon forest response to CO2 fertilization dependent on plant phosphorus acquisition. *Nat. Geosci.* 12, 736–741 (2019).
- Terrer, C. et al. Nitrogen and phosphorus constrain the CO2 fertilization of global plant biomass. Nat. Clim. Change 9, 684–689 (2019).
- Malhi, Y. et al. Exploring the likelihood and mechanism of a climate-change-induced dieback of the Amazon rainforest. Proc. Natl Acad. Sci. 106, 20610–20615 (2009).
- Zelazowski, P., Malhi, Y., Huntingford, C., Sitch, S. & Fisher, J. B. Changes in the potential distribution of humid tropical forests on a warmer planet. *Philos. Trans. R. Soc. Math. Phys. Eng. Sci.* 369, 137–160 (2011).
- 18. Huang, L. et al. Drought dominates the interannual variability in global terrestrial net primary production by controlling semi-arid ecosystems. Sci. Rep. 6, 24639 (2016).
- Castanho, A. D. A. et al. Potential shifts in the aboveground biomass and physiognomy of a seasonally dry tropical forest in a changing climate. *Environ. Res. Lett.* 15, 034053 (2020).
- Santoro, M. & Cartus, O. ESA Biomass Climate Change Initiative (Biomass\_cci): global datasets of forest above-ground biomass for the years 2010, 2017 and 2018, v3. NERC EDS Centre for Environmental Data Analysis https://doi.org/10.5285/5f331c418e9 f4935b8eb1b836f8a91b8 (2021).
- Baccini, A. et al. Tropical forests are a net carbon source based on aboveground measurements of gain and loss. Science 358, 230–234 (2017).
- 22. Harris, N. L. et al. Global maps of twenty-first century forest carbon fluxes. *Nat. Clim. Change* **11**, 234–240 (2021).
- Gatti, L. V. et al. Amazonia as a carbon source linked to deforestation and climate change. *Nature* 595, 388–393 (2021).
- Qin, Y. et al. Carbon loss from forest degradation exceeds that from deforestation in the Brazilian Amazon. Nat. Clim. Change 11, 442–448 (2021).
- Brienen, R. J. W. et al. Long-term decline of the Amazon carbon sink. Nature 519, 344–348 (2015).

- Hubau, W. et al. Asynchronous carbon sink saturation in African and Amazonian tropical forests. *Nature* 579, 80–87 (2020).
- 27. Phillips, O. L. et al. Drought sensitivity of the amazon rainforest. *Science* **323**, 1344–1347 (2009).
- 28. Ross, C. W. et al. Woody-biomass projections and drivers of change in sub-Saharan Africa. *Nat. Clim. Change* **11**, 449–455 (2021).
- 29. Larjavaara, M., Lu, X., Chen, X. & Vastaranta, M. Impact of rising temperatures on the biomass of humid old-growth forests of the world. *Carbon Balance Manag.* **16**, 31 (2021).
- Romps, D. M., Seeley, J. T., Vollaro, D. & Molinari, J. Projected increase in lightning strikes in the United States due to global warming. Science 346, 851–854 (2014).
- 31. Gora, E. M., Bitzer, P. M., Burchfield, J. C., Gutierrez, C. & Yanoviak, S. P. The contributions of lightning to biomass turnover, gap formation and plant mortality in a tropical forest. *Ecology* **102**, e03541 (2021).
- 32. Magnabosco Marra, D. et al. Windthrows control biomass patterns and functional composition of Amazon forests. *Glob. Change Biol.* **24**, 5867–5881 (2018).
- 33. Negrón-Juárez, R. I. et al. Windthrow variability in central amazonia. *Atmosphere* **8**, 28 (2017).
- 34. Silva Junior, C. H. L. et al. Persistent collapse of biomass in Amazonian forest edges following deforestation leads to unaccounted carbon losses. Sci. Adv. 6, 40 (2020).
- 35. Yin, Y. et al. Fire decline in dry tropical ecosystems enhances decadal land carbon sink. *Nat. Commun.* **11**, 1900 (2020).
- 36. Koch, A. & Kaplan, J. O. Tropical forest restoration under future climate change. *Nat. Clim. Change* **12**, 279–283 (2022).
- 37. Wang, S. et al. Recent global decline of  $CO_2$  fertilization effects on vegetation photosynthesis. *Science* **370**, 1295–1300 (2020).
- 38. Case, M. F. & Staver, A. C. Fire prevents woody encroachment only at higher-than-historical frequencies in a South African savanna. *J. Appl. Ecol.* **54**, 955–962 (2017).
- 39. Mau, A. C., Reed, S. C., Wood, T. E. & Cavaleri, M. A. Temperate and tropical forest canopies are already functioning beyond their thermal thresholds for photosynthesis. *Forests* **9**, 47 (2018).
- 40. Kolby Smith, W. et al. Large divergence of satellite and Earth system model estimates of global terrestrial CO2 fertilization. *Nat. Clim. Change* **6**, 306–310 (2016).
- 41. Martens, C. et al. Large uncertainties in future biome changes in Africa call for flexible climate adaptation strategies. *Glob. Change Biol.* **27**. 340–358 (2021).
- 42. Doughty, C. E. & Goulden, M. L. Are tropical forests near a high temperature threshold?. *J. Geophys. Res. Biogeosciences* **113**, G00B07 (2008).
- 43. Doughty, C. E. & Goulden, M. L. Seasonal patterns of tropical forest leaf area index and CO2 exchange. *J. Geophys. Res. Biogeosciences* **113**, GOOBO6 (2008).
- Langenbrunner, B., Pritchard, M. S., Kooperman, G. J. & Randerson, J. T. Why does amazon precipitation decrease when tropical forests respond to increasing CO2? *Earths Future* 7, 450–468 (2019).
- 45. Harris, I., Osborn, T. J., Jones, P. & Lister, D. Version 4 of the CRU TS monthly high-resolution gridded multivariate climate dataset. *Sci. Data* **7**, 109 (2020).
- Maurer, E. P., Brekke, L., Pruitt, T. & Duffy, P. B. Fine-resolution climate projections enhance regional climate change impact studies. EOS Trans. Am. Geophys. Union 88, 504–504 (2007).
- Reclamation. Downscaled CMIP3 and CMIP5 Climate and Hydrology Projections: Release of Hydrology Projections, Comparison with preceding Information, and Summary of User Needs. https://gdo-dcp.ucllnl.org/downscaled\_cmip\_projections/ techmemo/BCSD5HydrologyMemo.pdf (2014).

**Publisher's note** Springer Nature remains neutral with regard to jurisdictional claims in published maps and institutional affiliations.

Springer Nature or its licensor (e.g. a society or other partner) holds exclusive rights to this article under a publishing agreement with the author(s) or other rightsholder(s); author self-archiving

of the accepted manuscript version of this article is solely governed by the terms of such publishing agreement and applicable law.

@ The Author(s), under exclusive licence to Springer Nature Limited 2023

#### Methods

#### Climate data

We characterized the climate across the pantropical region from 1950 to 2099, divided into five -30-year timesteps. We refer to these periods as historic (1950–1979), current (1980–2009) and future (2010–2039, 2040–2069 and 2070–2099).

Climate data for the historic and current timeframes were obtained from the Climatic Research Unit (CRU) v.4.04 (ref.  $^{45}$ ) at  $0.5^{\circ} \times 0.5^{\circ}$  resolution. Future climate data were obtained from the CMIP5 multimodel ensemble, downscaled globally to  $0.5^{\circ}$  spatial resolution  $^{46,47}$ . We selected simulation results from 16 ESMs (Supplementary Table 1) for the RCP 4.5 and RCP 8.5 emission scenarios, corresponding to CO $_2$ e atmospheric concentrations of 650 and >1,000 ppm, respectively. Using the average precipitation and MCWD of the model simulations, we then estimated the future distribution of climate spaces and AGB changes. The upper and lower quartiles of the model simulations provided estimates of the uncertainty in AGB predictions, which arise from uncertainties in the climate predictions.

#### Climate space and AGB changes

We used an adapted version of the climatic space concept (defined in Malhi et al. 16 and Silva de Miranda et al. 48), which places pixels in a two-dimensional matrix defined by precipitation and MCWD. We then assigned an AGB value to each pixel to create a new 'bioclimatic space' concept that associates the original climate with its corresponding AGB. Within this matrix we defined seven climate categories, based on aridity index (AI) categories that strongly correlate with AGB content. Here, the AI is calculated as the ratio of precipitation and MCWD and classified based on a modified AI classification developed for use with the MCWD (Supplementary Table 2); we refer to these categories as climatic zones. MCWD is estimated as the maximum cumulative deficit between precipitation (that is, water supply) and potential evapotranspiration (PET, that is, water demand) within a year. As in Castanho et al. 19, we used the FAO-56 Penman–Monteith equation to estimate PET, available from the SPEI R package 49.

We estimated the average AGB (with confidence limits obtained through non-parametric bootstrapping) within each climatic zone using three AGB maps: Baccini et al.<sup>2</sup>, Xu et al.<sup>3</sup> and the European Space Agency (ESA) Biomass Climate Change Initiative dataset<sup>20</sup>. The Xu et al. and ESA AGB maps are from 2010, whereas the Baccini AGB data is based on satellite and light detection and ranging data for 2007–2008. To calculate the average AGB, we first excluded all pixels with anthropogenic land covers (croplands, herbaceous cover, mosaics where cropland or herbaceous cover was >50%, grasslands, and urban and bare areas), as mapped by the ESA land-cover change product for the year 2010. All other land-cover classes were included in our analysis. The result is an empirically based representation of the average AGB of natural vegetation throughout the tropical climate space. Average AGB density differs substantially among the various climatic zones. We then quantified changes in AGB based on the established relationships between AGB and climate. Moving from one climatic zone to another over time represents a shift in the equilibrium AGB. The equilibrium AGB of any pixel is assigned based on which climatic zone in the climate space it falls into in the historic and future climate scenarios. Pixels with at least 60% of their area covered by permanent water bodies were excluded from all analyses. We also used the ESA land-cover dataset to identify these water bodies.

#### **Uncertainty analysis**

The main sources of uncertainty in our final AGB and carbon predictions come from the CMIP5 climate predictions, the AGB climate model and the AGB datasets. To propagate the uncertainty from all of these sources, we generated 1,000 samples of future AGB for each pixel in each time frame. For each sample, we (1) randomly sampled a set of future climate conditions for each pixel to determine the

corresponding climatic zone; (2) selected one AGB dataset; and (3) sampled from the biomass distribution of the selected climatic zone based on the chosen biomass dataset. We used these samples to calculate the average and the variance in total AGB for each time frame.

#### Quantile regression forests and biomass changes

In addition to our discrete model, we used QRF to establish the relationship between AGB (from each dataset) and climate, and to predict future AGB under changing climate. The QRF were trained with the three AGB datasets mentioned earlier (Baccini et al.<sup>2</sup>, Xu et al.<sup>3</sup> and Santoro and Cartus (ESA)<sup>20</sup>), using precipitation and MCWD from the current period (1980-2009) as predictors. The forest size was 300 trees, with a minimum leaf node size of 10. The models showed good performance for both the training and validation data, with an  $R^2$ , coefficient of variation, from out-of-bag data of 0.82, 0.86 and 0.81 for the Baccini, Xu and ESA datasets, respectively. For predictions under the future climate, we built a QRF for each AGB dataset. QRF give the conditional quantiles of AGB predictions from random forests. Quantile random forests were used to estimate the distribution of AGB values for each combination of explanatory variables. To account for this uncertainty, we took random samples from these distributions when making predictions for changes in AGB. We used the  $R\,package\,ranger^{50}\,to\,fit\,the\,random\,forest\,and\,predict\,the\,quantiles.$ The figures presented in the main manuscript (Figs. 1–5) are from the discrete method, while results from the QRF approach are reported in the supplementary materials (Supplementary Tables 7 and 8 and Extended Data Figs. 1-4).

#### **Climatic zones**

The AI is a widely used numerical indicator of climatic water deficit, which is divided into five categories of aridity: hyperarid, arid, semiarid, dry subhumid and humid<sup>51</sup>. The thresholds for the climatic zones defined in this study (Supplementary Table 2) are modified from those defined in Middleton and Thomas<sup>51</sup> due to two key differences in our approach. First, the thresholds defined in AI (precipitation (P)/PET) were converted to P/water deficit (P/WD) (where WD is P - PET), so the climatic zones could be represented in our climatic space (precipitation versus MCWD). Second, we use the MCWD-a direct indicator of the intensity and length of the dry season-instead of the annual mean of water availability or water deficit. Finally, we divided the humid category into humid and humid seasonal zones. To separate large precipitation differences and depict a higher resolution of climatic characteristics, we further subdivided the modified humid category into a climatic zone with precipitation higher than 1,700 mm yr<sup>-1</sup> (that is, humid<sub>MAP>1,700</sub>) and another with precipitation lower than 1,700 mm yr<sup>-1</sup> (that is,  $humid_{MAP < 1,700}$  ). The precipitation threshold (1,700 mm  $yr^{-1}\!)$  $was \, defined \, based \, on \, previously \, published \, thresholds ^{17,52}, \, which \, vary \, defined \, based \, on \, previously \, published \, thresholds \, defined \, based \, on \, previously \, published \, thresholds \, defined \, based \, on \, previously \, published \, thresholds \, defined \, based \, on \, previously \, published \, thresholds \, defined \, based \, on \, previously \, published \, thresholds \, defined \, based \, on \, previously \, published \, thresholds \, defined \, based \, on \, previously \, published \, thresholds \, defined \, based \, on \, previously \, published \, thresholds \, defined \, based \, on \, previously \, published \, thresholds \, defined \, based \, defined \, based \, defined \, based \, defined \, based \, defined \, d$ between 1,500-2,000 mm yr<sup>-1</sup>.

## Data availability

CRU v.4.04 data can be downloaded from the CRU website (https://crudata.uea.ac.uk/cru/data/hrg/). Downscaled climate data from the Coupled Model Intercomparison Project Phase 5 (CMIP5) multimodel ensemble can be downloaded from https://gdo-dcp.ucllnl.org/downscaled\_cmip\_projections/dcpInterface.html. Global biomass data is available from https://developers.google.com/earth-engine/datasets/catalog/WHRC\_biomass\_tropical)², https://doi.org/10.5281/zenodo.4161694 (ref.³) and https://catalogue.ceda.ac.uk/uuid/5f331c418e9f4935b8eb1b836f8a91b8 (ref.²0). MODIS Land Cover data is available at https://lpdaac.usgs.gov/products/mcd12q1v006/. Continent borders are from the Environmental Systems Research Institute's World Continents shapefiles v.10.3 (http://gis.ucla.edu/geodata/dataset/continent\_In)<sup>53</sup>. Preprocessed input data (as specified in the manuscript), partial results and final predictions of changes in area and biomass are available in a public repository via Dryad<sup>54</sup>.

## **Code availability**

Relevant R scripts used to process the data and perform the analyses are available in a public repository via Dryad<sup>54</sup>.

#### References

- Silva de Miranda, P. L. et al. Using tree species inventories to map biomes and assess their climatic overlaps in lowland tropical South America. Glob. Ecol. Biogeogr. 27, 899–912 (2018).
- Beguería, S., Vicente-Serrano, S. M., Reig, F. & Latorre, B. Standardized precipitation evapotranspiration index (SPEI) revisited: parameter fitting, evapotranspiration models, tools, datasets and drought monitoring. *Int. J. Climatol.* 34, 3001–3023 (2014)
- 50. Wright, M. N. & Ziegler, A. ranger: a fast implementation of random forests for high dimensional data in C++ and R. J. Stat. Softw. 77, 1–17 (2017).
- Middleton, N., Thomas, D. & UNEP. World Atlas of Desertification (Arnold, 1997).
- 52. Staver, A. C., Archibald, S. & Levin, S. A. The global extent and determinants of Savanna and forest as alternative biome states. *Science* **334**, 230–232 (2011).
- 53. ESRI Data & Maps. World Continents Version 10.3. (2015).
- Uribe, M. R. et al. Net loss of biomass predicted for tropical biomes in a changing climate. Dryad https://doi.org/10.7280/ D1D124 (2023).

#### **Acknowledgements**

We acknowledge the World Climate Research Programme's Working Group on Coupled Modelling, which is responsible for CMIP, and we thank the climate modelling groups (listed in Supplementary Table 4) for producing and making available their model outputs. For CMIP, the U.S. Department of Energy's Program for Climate Model Diagnosis and Intercomparison provided coordinating support and led development of software infrastructure in partnership with the Global Organization for Earth System Science Portals. This research was supported through funding from the National Science Foundation (MSB-ECA award no. 1802754: INFEWS/T1 award no. 1739724).

#### **Author contributions**

M.T.C., M.N.M. and P.M.B. conceived the study. M.R.U. and A.D.A.C. performed the data analysis and prepared the manuscript. P.M.B. and D.V. contributed to the data processing and analysis. All the authors contributed and edited the manuscript.

## **Competing interests**

The authors declare no competing interests.

#### **Additional information**

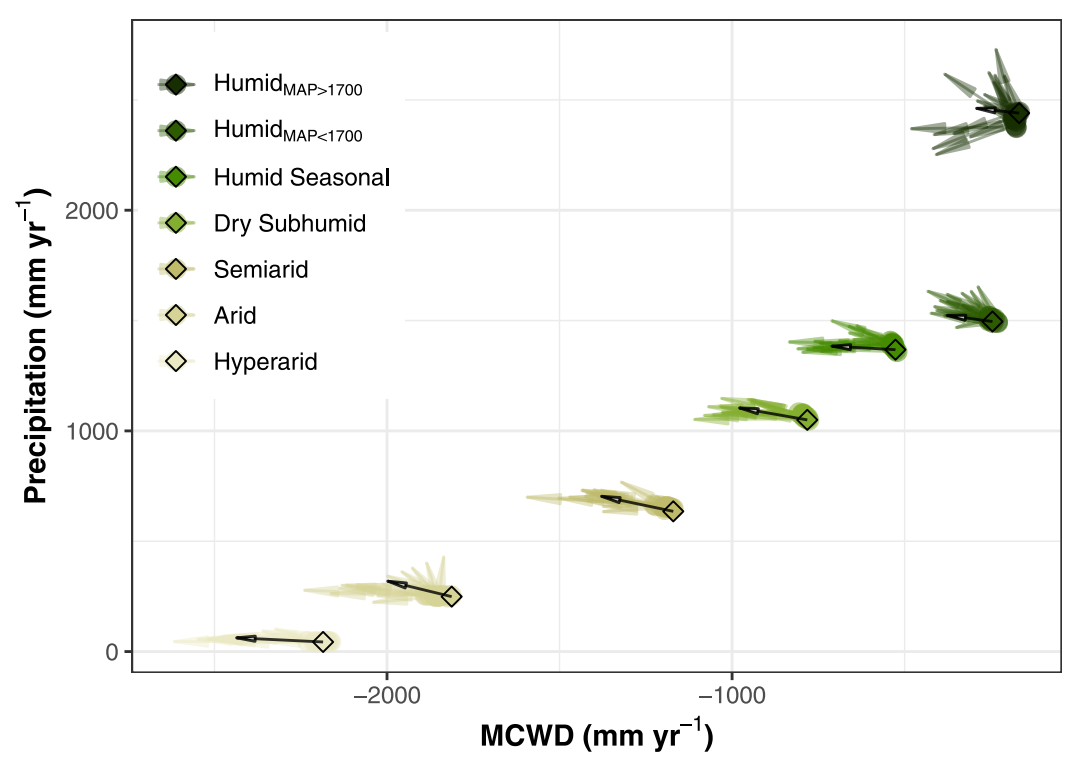
**Extended data** is available for this paper at https://doi.org/10.1038/s41558-023-01600-z.

**Supplementary information** The online version contains supplementary material available at https://doi.org/10.1038/s41558-023-01600-z.

**Correspondence and requests for materials** should be addressed to Maria del Rosario Uribe or Paulo M. Brando.

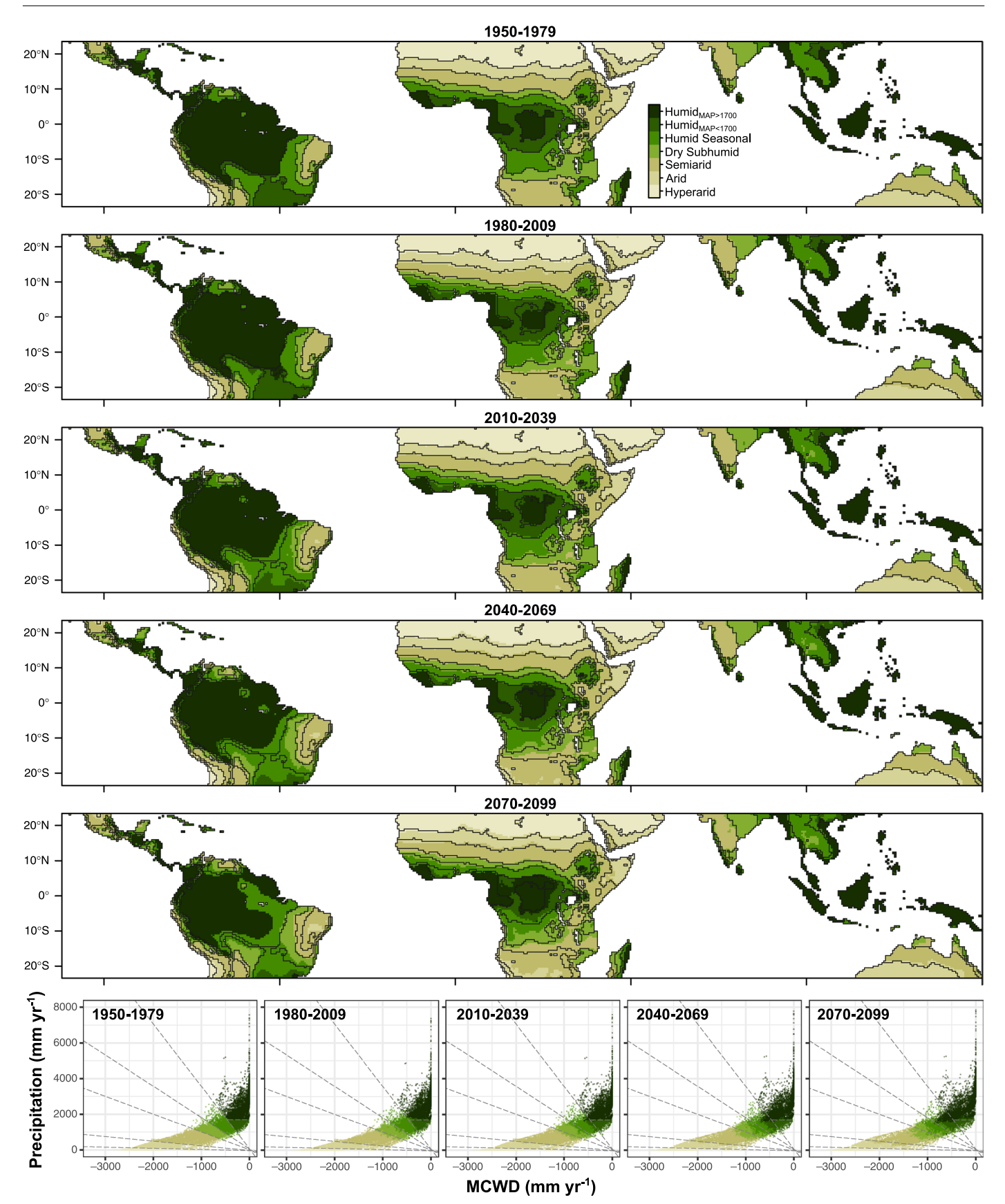
**Peer review information** *Nature Climate Change* thanks Manan Bhan and the other, anonymous, reviewer(s) for their contribution to the peer review of this work.

**Reprints and permissions information** is available at www.nature.com/reprints.



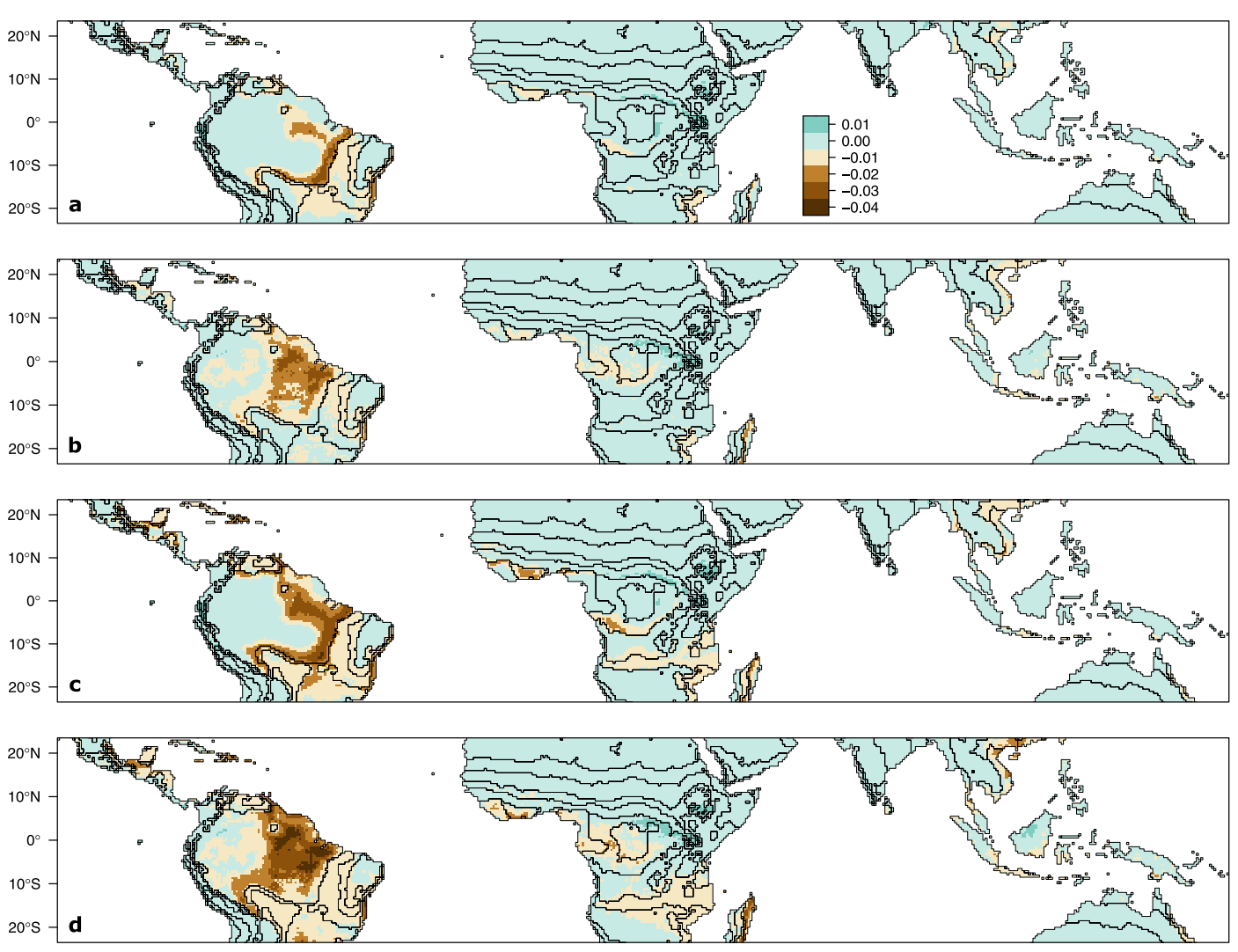
Extended Data Fig. 1 | Distribution of climatic zones in the tropics for Historic and Future 30-year time periods (1950–1979, 1980–2009, 2010–2039, 2040–2069, and 2070–2099). Colors represent the climatic zones. Contour lines in the maps and gray dashed lines in the scatterplots are plotted for

reference to show the distribution and limits of the climatic zones in the period 1950–1979. Climate data from CRU v.4.04  $^{45}$  for 1950–2009 and from CMIP5 projections  $^{46,47}$  for 2010–2099 under RCP 8.5.

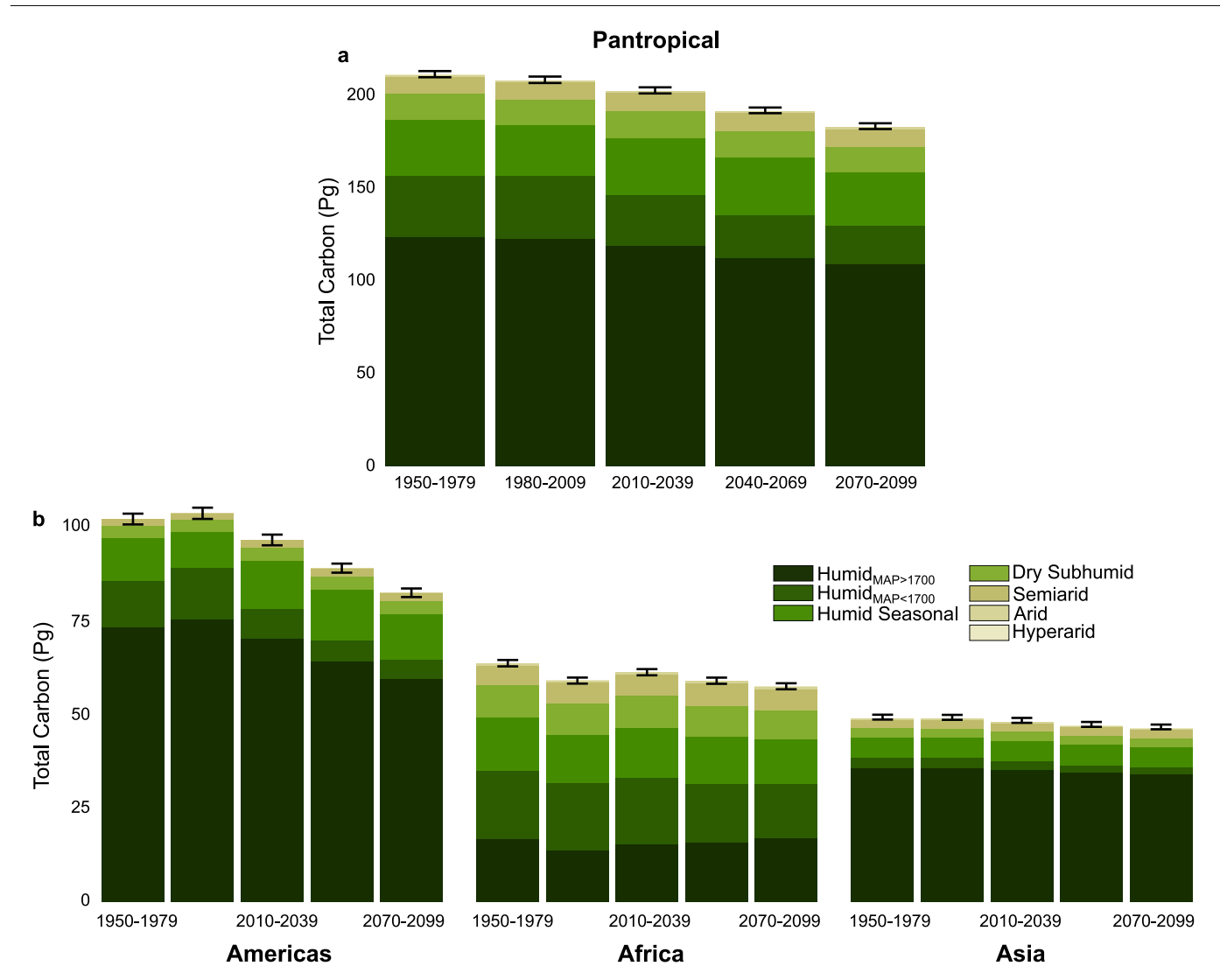


Extended Data Fig. 2 | Individual model projections of precipitation and MCWD under RCP 8.5. Dots represent each model's mean Historic (1950–1979) climate for each climatic zone. Connected arrowheads represent average climate at the end of the century (2070–2099). The black shapes correspond to the

average climate from all models. Models used are listed in Supplementary Table 1. Climate data from CRU v.4.04 $^{45}$  for 1950–2009 and from CMIP5 projections  $^{46,47}$  for 2010–2099 under RCP 8.5.



**Extended Data Fig. 3** | **Biomass and biomass changes across the tropics under all scenarios.** Changes in carbon (Pg) in the tropics by pixel predicted from (a, c) our climatic zone averaging method and (b, d) quantile regression forest from 1950–2099. Climate data from CRU  $4.04^{45}$  for 1950–2009 and from CMIP5 projections  $^{46,47}$  for 2010–2099 under RCP 4.5 (a, b) and RCP 8.5 (c, d).



**Extended Data Fig. 4** | **Changes in carbon (Pg) in the tropics under RCP 8.5.** Changes in carbon (Pg) by climatic zone from 1950–2099 for the entire tropics (a) and for each region (b). Climate data from CRU  $4.04^{45}$  for 1950–2009 and from CMIP5 projections  $^{46,47}$  for 2010–2099 under RCP 8.5.